Remote Sensing of Environment 113 (2009) 2052–2061

Contents lists available at ScienceDirect

Remote Sensing of Environment

journal homepage: www.elsevier.com/locate/rse

Integrating SPOT-5 time series, crop growth modeling and expert knowledge for monitoring agricultural practices — The case of sugarcane harvest on Reunion Island

Mahmoud El Hajj [a,*], Agnès Bégué [b], Serge Guillaume [c], Jean-François Martiné [d]

[a] Cemagref, UMR TETIS, Montpellier, F-34093 France
[b] CIRAD, UMR TETIS, Montpellier, F-34093 France
[c] Cemagref, UMR ITAP, Montpellier, F-34196 France
[d] CIRAD, UR SCA, Saint-Denis, La Réunion, F-97408 France

ARTICLE INFO

Article history:
Received 24 June 2008
Received in revised form 2 April 2009
Accepted 11 April 2009

Keywords:
Multi-temporal
Change detection
Mutli-source
Fusion
Fuzzy
NDVI
Cropping system

ABSTRACT

Time series of optical satellite images acquired at high spatial resolution is a potentially useful source of information for monitoring agricultural practices. However, the information extracted from this source is often hampered by missing acquisitions or uncertain radiometric values. This paper presents a novel approach that addresses this issue by combining time series of satellite images with information from crop growth modeling and expert knowledge. In a fuzzy framework, a decision support system that combines multi-source information was designed to automatically detect the sugarcane harvest at field scale. The formalism that we used deals with the imprecision of the data and the approximation of expert reasoning. System performances were analyzed using a time series of SPOT-5 images. Results obtained were in substantial agreement with ground truth data: overall accuracy reached 97.80% with stability values exceeding 89.21% for all decisions. The contribution of fuzzy sets to overall accuracy reached 15.08%. The approach outlined in this paper is very promising and could be very useful for other agricultural applications.

1. Introduction

Time series of satellite images are a cost effective, high quality source of data to assess land cover dynamics and to monitor changes in large areas. The synergetic use of this source and advanced analytical methods enables complex problems related to a wide range of agricultural and environmental applications to be solved (Bruzzone & Smits, 2002).

In the past decade, several studies have reported the potential of time series of large scale satellite observations such as AVHRR (Advanced Very High Resolution Radiometer), MODIS (Moderate Resolution Imaging Spectroradiometer), MERIS (Medium Resolution Imaging Spectrometer) and SPOT-Vegetation, for monitoring vegetation (Beck et al., 2006; Boles et al., 2004; Gobron et al., 2005; Maignan et al., 2008; McCloy & Lucht, 2004). However, because of the coarse spatial resolution of the images, these studies only dealt with global structures.

Now a new generation of time series acquired at high spatial resolution is available thanks to repetitive acquisitions by satellites such as SPOT 4/5, Landsat 5/7 and Formosat 2. This new generation allows changes in land cover to be detected and monitored at a much finer spatial scale. Several authors have recognized the benefits of this kind of data for classifying land cover (Baldi et al., 2006; Murthy et al., 2003; Pax-Lenney & Woodcock, 1997; Turner & Congalton, 1998), identifying crops (Guerif et al., 1996), mapping seasonal patterns and crop rotations (Martinez-Casasnovas et al., 2005; Panigrahy & Sharma, 1997), monitoring harvest and planting (Lebourgeois et al., 2007), mapping forests (Vagen, 2006; Woodcock et al., 2001), and for many other topics, as shown in papers collected in (Bruzzone & Smits, 2002; Smits & Bruzzone, 2004).

Nevertheless, the content of the information extracted from high spatial resolution time series is often limited by gaps in image acquisition due to clouds and/or image programming capacity, and by the uncertainty and the imprecision of the radiometric value due to atmospheric conditions and radiometric calibration. To make credible decisions, such information thus needs to be supplemented with data from other sources and, in addition, the data must be integrated in a system that can deal with imprecision and uncertainty.

In recent years, several studies have been oriented towards data fusion approaches that operate jointly various remote sensing sources. These sources include images from multiple sensors with different or identical resolutions (spatial, spectral and temporal), e.g. Hyde et al. (2006), as well as data derived from remote sensing images by mathematical operations or transforms, e.g. Le Hégarat-Mascle and Seltz (2004). In Hyde et al.

* Corresponding author. Fax: +33 4 6754 8700.
E-mail addresses: mahmoud.elhajj@teledetection.fr (M. El Hajj), agnes.begue@cirad.fr (A. Bégué), serge.guillaume@montpellier.cemagref.fr (S. Guillaume), jean-francois.martine@cirad.fr (J.-F. Martiné).

0034-4257/$ – see front matter © 2009 Elsevier Inc. All rights reserved.
doi:10.1016/j.rse.2009.04.009

(2006), the authors integrated structural information from LiDAR, radar (SAR/InSAR) and optical (Landsat ETM+, Quickbird) images to improve mapping of forest structure. They have shown that the integration of ETM+ data improves considerably estimates from LiDAR data and that the contributions of radar and Quickbird data are marginal. In Le Hégarat-Mascle and Seltz (2004), a method that combines different indices calculated from multi-temporal imagery was developed to evaluate forest damage. This method was then used in different applications with SPOT HRV images, for example, forest logging in either pine or mixed forests, or the vegetation cover of fields in intensive farming areas in winter (Le Hegarat-Mascle et al., 2006).

Remote sensing data were also integrated with information from other sources that have different natures; they have been integrated with expert knowledge, e.g. Lobell et al. (2003), ancillary data, e.g. Lucas et al. (2007) and agronomic or ecosystem models, e.g. Yan et al. (2007). The purpose of integration varied from one application to another. In Lobell et al. (2003), knowledge about crop phenology was combined with Landsat TM/ETM+ multi-temporal imagery to estimate regional crop rotation. In Lucas et al. (2007), the use of Landsat ETM+ time series acquired over an annual cycle was evaluated for the mapping of semi-natural habitats and agricultural land cover by integrating topographic maps, digital elevation data, digital orthophotography, and other supportive data. Data from NOAA/AVHRR images have been combined, in Yan et al. (2007), with an ecosystem model to estimate the potential for carbon sequestration in agricultural soils and to assess the sustainability of soil carbon uptake under different soil management modes.

Integrating remote sensing data with agronomic models (e.g. assimilation, forcing, etc.) has been widely used to estimate crop growth status and to improve yield prediction (Delecolle et al., 1992; Guerif & Duke, 2000; Launay & Guerif, 2005). The benefit of integration has always been improvement in the performance of the agronomic model (Moulin et al., 1998). Up to now, little attention has been paid to the use of the outputs of agronomical models as a source of information to help analyze remote sensing data. Based on climatic and soil biophysical parameters, these models could provide useful information to compensate for the lack of radiometric data from satellite time series.

Another substantial source of information is expert knowledge about the agricultural application concerned (Middelkoop & Janssen, 1991); this source enables automation of the analysis of radiometric data, and provides very useful information in the case of gaps in image acquisition.

The aim of this paper is to present a novel approach to detect change using time series of satellite images that integrates information from crop growth modeling and expert knowledge. To our knowledge, this approach has never before been used and will be useful for monitoring agricultural practices, particularly, crop harvest.

To illustrate our approach, we describe its application for the detection of sugarcane harvest using a SPOT-5 time series. The sugarcane cropping system is of particular interest because of the very high spatio-temporal variability of the fields; the sugarcane harvest campaign lasts several months, which makes it difficult to monitor fields when satellite time series include acquisition gaps. A decision support system designed and implemented to address this issue is presented here.

Because of its well known ability to deal with imprecise and uncertain information, and to model linguistic concepts, fuzzy logic formalism was chosen to design the decision support system. Moreover, thanks to fuzzy inference, it is able to assign a confidence factor to each decision.

2. Agricultural application

Every year, about 20 million hectares of sugarcane are harvested (FAOSTATS[1], 2007) in more than 100 tropical countries. The world cropped area is increasing steadily due to growing consumption of sugar in developing countries and to the emerging bio-energy markets.

Sugarcane is a semi-perennial grass that belongs to the "Graminae" family and propagates vegetatively. The planting material used is stem cuttings. After the plant crop is harvested (between approximately 18 and 24 months of age), buds on remaining underground stubble germinate again and give rise to another crop. This crop is called the ratoon crop, and is harvested about every 12 months for up to four years or more, when the crop is renewed due to decreasing yield. The crop is harvested when it is fully mature and ripe. Early varieties and ratoon crops are the first to be harvested after the mill opens. The harvest season generally lasts several months, depending on the tonnage of cane to be processed, the capacity of the mills, and the climate.

One of the main needs expressed by the sugarcane industry worldwide is to obtain information on the progress of harvest throughout the harvest season, which generally lasts between four and eight months. When information is available over large areas, it can help improve the organization of the harvest campaign, thereby increasing work efficiency in both the field and the factory. Time series of satellite images are a promising way to meet this need.

Several investigators have reported the capacity of multi-temporal imagery in monitoring sugarcane harvest (Bégué et al., 2004; Gers & Schmidt, 2001; Lebourgeois et al., 2007). In Gers and Schmidt (2001), the authors used four SPOT-4 images to detect the harvested fields in a region of South Africa with an accuracy that ranges from 62% to 85%; they reported some limitations related to the spatial resolution of the images that sometimes is not suitable for small plots. In Bégué et al. (2004), the potential of a SPOT-4 and 5 time series (four images) for detecting and estimating harvested surfaces in Guadeloupe was studied; the obtained results were rather encouraging with 90% of well classified pixels. In Lebourgeois et al. (2007), three SPOT images were used to map the sugarcane harvested fields on Reunion Island with an overall accuracy between 93.8% and 96.5% and a harvest detection accuracy that reaches 89.5%; the number of fields involved in this study was small and the results were only evaluated on the zones that are cloud-free in all the images simultaneously.

The main method proposed in the literature for monitoring sugarcane harvest is based on multi-spectral classification combined with visual interpretation. In spite of the good performances obtained in some studies, e.g. Lebourgeois et al. (2007), this method has two major drawbacks:

- The subjective and time-consuming photo-interpretation stage needed (i) to reduce the number of classes resulting from an unsupervised classification, (ii) or to choose the learning samples required to perform a supervised classification;
- The radiometric confusion between different classes due to the fact that the sugarcane harvest campaign lasts several months. When the interval between two cloud-free images is too long, it is difficult to differentiate between a standing crop and the regrowth in a field harvested at the beginning of the season.

There was thus a need to develop and implement an automatic and a robust method that, in addition to satellite-image time series, relies on information from other sources.

3. Theoretical background of fuzzy inference systems

Fuzzy set and possibility theories (Zadeh, 1965, 1978) began appearing in the remote sensing literature about 20 years ago. The main use of fuzzy systems has been in image segmentation and classification, e.g. Gopal et al. (1999), Li et al. (2007), Tapia et al. (2005), as well as in the implementation of fuzzy assessment indices, e.g. Gill et al. (2000), Laba et al. (2008), based on the pioneer work of Woodcock and Gopal (2000).

[1] http://faostat.fao.org/.

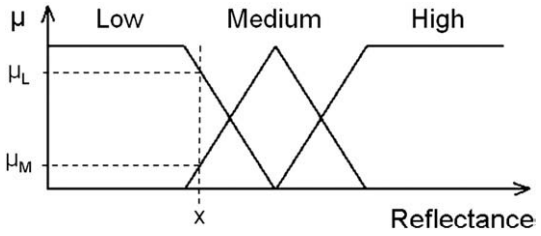

Fig. 1. A standardized fuzzy partition of reflectance.

The decision support system we describe in this paper is a Fuzzy Inference System (FIS). The goal of this section is not to provide an extensive introduction to fuzzy logic (see Bouchon-Meunier & Marsala, 2003; Dubois & Prade, 2000; Zadeh, 1965), but only to provide the reader with some theoretical background on FIS and a brief description of fuzzy linguistic modeling.

FIS are one of the most famous applications of fuzzy logic and fuzzy set theory (Guillaume, 2001). The strength of FIS lies in their twofold identity: on the one hand they are able to handle linguistic concepts such as High or Low; on the other hand, they are universal approximators able to perform non-linear mapping between inputs and outputs. The non-linear mapping process can be done through automatic learning procedures, keeping in mind the originality of fuzzy logic, i.e. its interpretability (Guillaume, 2001). This means that optimization and other automatic procedures must preserve the semantic expressivity of the fuzzy sets and the rules.

A fuzzy set is defined by its membership function. A point in the universe, x, belongs to a fuzzy set, A, with a membership degree, $0 \leq \mu_A(x) \leq 1$. Fuzzy sets can be used to model linguistic concepts. If A is a set of *High* reflectance values, the membership degree of a given reflectance value, x, $\mu_A(x)$, can be interpreted as the level up to which the x reflectance should be considered as *High*. Several fuzzy sets, e.g. *Low*, *Medium* and *High*, can be defined in the same universe of variable partition, as illustrated in Fig. 1.

As fuzzy sets usually overlap, a data point is likely to belong to more than one fuzzy set. In the partition shown in Fig. 1, the value x belongs to the fuzzy sets *Low* and *Medium* with the corresponding membership degrees μ_L and μ_M. It should be underlined that with such partitions, a given point may belong, with a non null degree, to at most two fuzzy sets. Moreover, for each point in the universe, the sum of the membership degrees to all the fuzzy sets of the partition is normalized to one.

Fuzzy sets are used in a FIS to build linguistic rules, for instance "If reflectance is High then …". For an x value of reflectance, the matching degree of the rule, w, which means how true the rule is for the example, is given by the membership degree of x to the fuzzy set *High*, $\mu_H(x)$. Usually several variables are involved in the description of the rule. The rth rule in the FIS rule base is written as follows:

$$\text{If } x_1 \text{ is } A_1^r \text{ and } x_2 \text{ is } A_2^r \ldots \text{and } x_p \text{ is } A_p^r \text{ then } y \text{ is } C^r \tag{1}$$

where A_k^r is the fuzzy set of the k^{th} input variable used within the r^{th} rule and C^r is the rule conclusion.

Thanks to fuzzy set overlap in the universe, a given input is likely to fire several rules. Consequently, these rules will be involved in the system inference. The inference method defines the way in which the system attributes weights to the conclusions of fired rules and the way it aggregates the weighted conclusions of these rules to take them all into account.

In this study, the weight w^r attributed to the conclusion C^r of an activated rule r is calculated by combining the membership degrees of rule premises in a conjunctive way as follows:

$$w^r(C^r) = \mu_{A_1^r}(x_1) \wedge \mu_{A_2^r}(x_2) \wedge \ldots \wedge \mu_{A_p^r}\left(x_p\right) \tag{2}$$

where $\mu_{A_j^r}(x_j)$ is the membership degree of the x_j value to the fuzzy set A_j^r, and $\wedge$ a conjunctive operator, the *min* and the *product* being the most commonly used ones.

The aggregation of the m distinct conclusions is done in a disjunctive way as follows:

$$\begin{cases} \forall j = 1, \ldots, m \\ \mu_j = \left\{ \underset{r}{\vee} (w^r(C^r)) \,|\, C^r = j \right\} \end{cases} \tag{3}$$

where $\vee$ is a disjunctive operator, e.g. the max.

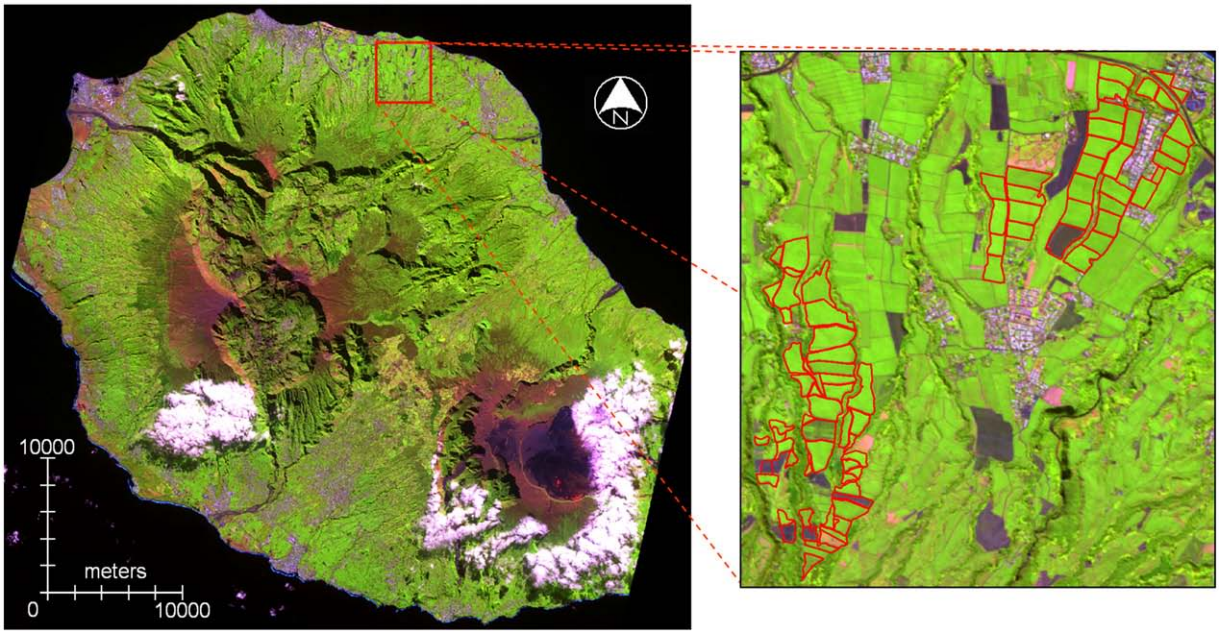

Fig. 2. On the left, a false color composite (Red: band-4; Green: band-3; Blue: band-1) of a SPOT5 image acquired over Reunion Island on May 13, 2004 (© CNES, Distribution Spot Image). On the right, a closer view of the study site with the sugarcane fields in the study outlined in red. (For interpretation of the references to colour in this figure legend, the reader is referred to the web version of this article.)

Table 1
Characteristics of the SPOT5 time series.

Dates	SPOT5 instrument	Incidence angle (in degree) (right = −)	Solar elevation (in degree)	Phase angle (in degree)
01/10/2003	HRG 2	−04.65	64.10	21.28
02/26/2003	HRG 1	−11.94	58.54	22.07
04/24/2003	HRG 1	−04.39	48.02	40.23
05/04/2003	HRG 1	+10.90	46.80	47.99
07/21/2003	HRG 1	+10.58	41.20	53.13
08/21/2003	HRG 1	+18.17	48.90	51.00
09/01/2003	HRG 1	−04.42	50.63	37.31
10/08/2003	HRG 1	−25.95	60.40	19.75
12/19/2003	HRG 1	−02.90	67.20	19.90
03/17/2004	HRG 2	−19.10	54.2	25.24
04/11/2004	HRG 1	+17.95	52.45	48.41
05/13/2004	HRG 1	−11.80	42.90	43.86
06/18/2004	HRG 2	+03.25	39.10	51.95
07/09/2004	HRG 1	−04.73	38.83	49.70
08/19/2004	HRG 1	+17.96	48.50	51.24
10/26/2004	HRG 2	+03.30	67.90	24.94
11/06/2004	HRG 1	−19.16	66.63	09.07
12/07/2004	HRG 1	−12.28	66.65	11.19

The output of the system is the membership degree μ_j assigned to each possible conclusion j.

4. Materials

4.1. Study site

The study site is located in north-eastern Reunion Island (Fig. 2), a small territory of around 2500 km^2 which is an overseas department of France in the Indian Ocean (21°7′ to 19°40′ S, 55°13′ to 61°13′ E), east of Madagascar. The site contains two sugarcane farms: the first located at an altitude of around 70 m and comprising 33 fields with an average size of 5.4 ha, the second located at an altitude ranging from 400 to 700 m, with 46 fields with an average size of 3.47 ha. As the study area is in the tropics, the year is divided into two seasons: a hot, rainy season from November to April, and a cool, dry season from May to October.

4.2. Data sets

The satellite data set used in this study consisted of 18 SPOT-5 images acquired over Reunion Island between January 10, 2003 and December 7, 2004. Both HRG1 and HRG2 SPOT-5 instruments acquire radiation in four spectral bands with high spatial resolution: 10 m in Green, Red and Near Infra-Red (NIR) bands, and 20 m in Short Wave Infra-Red (SWIR) band. The images belong to the KALIDEOS database set up by the CNES[2] (CNES, 2007; DeBoissezon & Sand, 2006). All images were orthorectified and coregistered to the UTM coordinate system (zone 40 South) with a root mean square error of less than 0.5 pixel per image.

The radiometry of the images was atmospherically corrected using the 6S code, so that pixel values represented top of canopy reflectances (TOC) in the four spectral bands. Since no in situ radiometric measurements were available, the validation of the TOC reflectances was performed by comparing them to the output of a relative radiometric normalization method (El Hajj et al., 2008). Due to the imperfections of the radiometric correction, satellite images were considered as a potential source of imprecision and uncertainty. Cloud and saturated-pixel masks were available for each image. Table 1 shows the characteristics of the images in the time series.

Block plot boundaries for the whole of Reunion Island were provided by DAF[3] services, and refined to define the boundaries of each field at the study site (Lebourgeois et al., 2007).

Daily climatic data recorded at two meteorological stations, La Mare and Bagatelle, located near the two sugarcane farms (Source: Meteorological Data Base of CIRAD[4] in Reunion) were used to run the crop growth model during the period covered by the satellite time series. These data are daily estimations of rainfall (mm), potential evapotranspiration (mm), global radiation (J/m^2), and minimum, maximum, and mean temperature (°C).

A ground truth database was built by using harvest dates reported by farmers for each field during the 2003 and 2004 harvest campaigns covered by the satellite acquisitions. This database gives the status of each sugarcane field (whether it has been harvested or not) between each pair of consecutive images in the time series.

5. Method

In this section we first present the sources from which information was extracted to feed the decision support system, and then describe its components, and finally show how it was used to make decisions for use with sugarcane.

5.1. Information extraction

5.1.1. Time series of satellite images

The time series of SPOT-5 images were the main source of information. Using field boundaries and images, a temporal profile of NDVI (Normalized Difference Vegetation Index) was calculated for each field at the study site, at field scale:

$$\mathrm{NDVI} = \frac{\rho_{\mathrm{NIR}} - \rho_{\mathrm{red}}}{\rho_{\mathrm{NIR}} + \rho_{\mathrm{red}}} \quad (4)$$

where ρ_{red} and ρ_{NIR} are reflectances in the red and NIR bands.

This calculation was done after eliminating mixed border pixels of fields and after discarding saturated and cloud-contaminated pixels using cloud and saturation masks. The saturation in some spectral bands of some images was due to problems with the gain tuning of the satellite sensors.

The NDVI temporal profile of sugarcane field provides useful information about the current status of the field and the different historical stages. In general, this profile can be divided into two periods: a period in which NDVI values increase, corresponding to the vegetative development of the sugarcane, and another period with steady or decreasing values, corresponding to the mature phase of the plant. Fig. 3 shows an example of the temporal profile of NDVI for ratoon and planted crops (see Section 5.1.3). Since the sugarcane harvest lasts several months, the temporal profile of NDVI may shift in time from one field to another, and in addition, the length of the growing period of a late crop is generally shorter than that of an early crop.

The information extracted from the temporal profile of the NDVI suffers from two major limitations: the lack of image acquisitions and the imprecision. NDVI temporal profiles are often incomplete because of gaps in image acquisition, atmospheric conditions and/or radiometric problems. Filling gaps in these profiles is not an easy issue. The difficulty is due to the high spatio-temporal variability of sugarcane fields that induces a high variability in the NDVI temporal profiles (Bégué et al., Accepted for publication). The length of the harvest campaign (about 6 months) leads to significant phenological changes between fields and to different environmental conditions of sugarcane

[2] *Centre National d'Etudes Spatiales* (French Space Agency).

[3] *Direction de l'Agriculture et de la Forêt* (Directorate of Agriculture and Forestry).

[4] *Centre de coopération internationale en recherche agronomique pour le développement* (French Agricultural Research Centre for International Development).

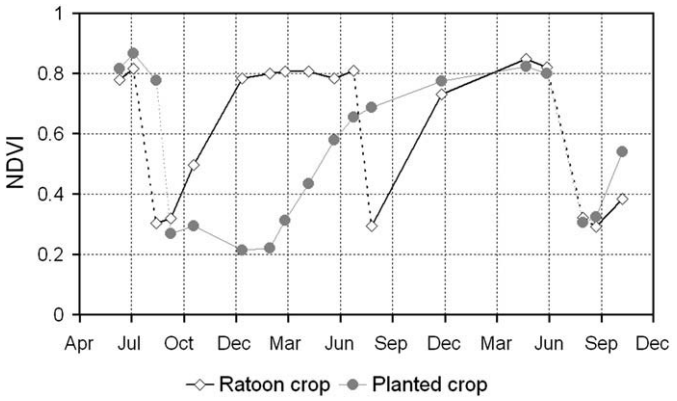

Fig. 3. Example of the temporal profile of two types of sugarcane NDVI: ratoon crop and planted crop.

regrowth after the harvest. Other sources of information that consider the environmental and temporal conditions are thus required to cope with the gaps and to help detecting field harvest. The second limitation, the imprecision, is basically due to the imperfections of the radiometric corrections. To address this limitation one should work with symbolic data, i.e. qualitative data, rather than numeric data.

5.1.2. Crop growth modeling

Model simulations of crop growth based on climatic data and soil characteristics were the second source of information. This source was used to simulate NDVI temporal profiles to build a synthetic variable that is independent of the time series and that is able to provide information about the possibility of sugarcane being harvested between two specific dates.

We used the sugarcane ecophysiological growth model MOSICAS (Martiné & Todoroff, 2002) to simulate sugarcane growth in each field at the study site at a daily time scale. MOSICAS, a thermoradiative-type model that accounts for water stress, consists in growth and carbon balance modules linked to a water balance module. Among other output state variables, MOSICAS simulates the leaf area index (LAI) of a sugarcane field. The modeling of LAI is of the 'big leaf' type, and is based on the balance between daily increase (growth) and daily decrease (senescence) in leaf surface area. This balance is mainly driven by temperature and is limited by radiation with respect to leaf mass and water stress.

Since our aim was to acquire information based on the NDVI, we transformed daily estimations of LAI into daily estimations of NDVI using the regression model (Eq. (5)) previously described in El Hajj et al. (2007).

$$\mathrm{NDVI} = 1 / 9.713 \times ln(\mathrm{LAI} / 0.003) \quad (5)$$

This regression model ($R^2 = 0.92$) was established using in situ LAI measurements performed in 2002 and 2003 on different sugarcane fields on Reunion Island (R570 and R579 varieties) and SPOT NDVI values interpolated at measurement dates. All the data used were acquired during the growth phase of ratoon crops (before and during the period of maximum NDVI); therefore the regression model is only valid for the green LAI. As the fields are covered with straws after the harvest, the soil type does not influence the model.

From the simulated NDVI temporal profiles, we built a helpful indicator for harvest detection: Tn that represents the nominal time (in number of days) for a sugarcane field NDVI to reach a given threshold starting with a "supposed" harvest date.

Fig. 4 illustrates an example of relationships between Tn and the "supposed" harvest date, for different NDVI threshold values. According to this example, to reach an NDVI of 0.7, sugarcane will need 133 days (Tn = 133) of growth if harvested in early July (during the cool, dry season) but only 89 days (Tn = 89) if harvested early December (during the hot, rainy season). We observed that for high NDVI thresholds (0.7 in our example) the model is very sensitive to climatic variations, such as rainfall amount.

The indicator extracted from crop growth modeling, mainly based on climatic data, gives information about the possibility of a sugarcane field being harvested between two satellite acquisition dates. This information is particularly useful when the interval between two cloud-free images is long (e.g. more than 2 months).

5.1.3. Expert knowledge

Knowledge about the phenological stages of sugarcane, as well as about its cropping systems (c.f. Section 2), is crucial information that must be integrated in the decision support system. This source enables a better understanding of the relationship between the temporal behavior of NDVI and the crop field status, and provides important temporal constraints that ease decisions in the case of missing radiometric data. Examples of parameters defining these temporal constraints are the nominal cycle length of the sugarcane, and mill opening and closing dates which determine the harvest campaigns.

Expert knowledge is involved in different parts of the decision support system. It is used:

(1) to define the input variables needed to automatically detect the sugarcane harvest;
(2) to configure the partitions (i.e., fuzzy sets) of these variables;
(3) to integrate useful information about the sugarcane cycle, and
(4) to define the inference rules.

5.2. Decision support system

The decision support system provides information about the possibility of a sugarcane field being harvested between two acquisition dates t and t'.

5.2.1. System inputs

The system has 11 inputs that are built using information extracted from the three different sources: time series of SPOT-5 images (TS), crop growth modeling (CM), and expert knowledge (EK).

The first set of inputs {In1, In2, In3, In4, In5} concerns temporal information, the second set {In6, In7, In8} NDVI values, and the third set {In9, In10, In11} NDVI dynamics. Table 2 shows the characteristics of each input.

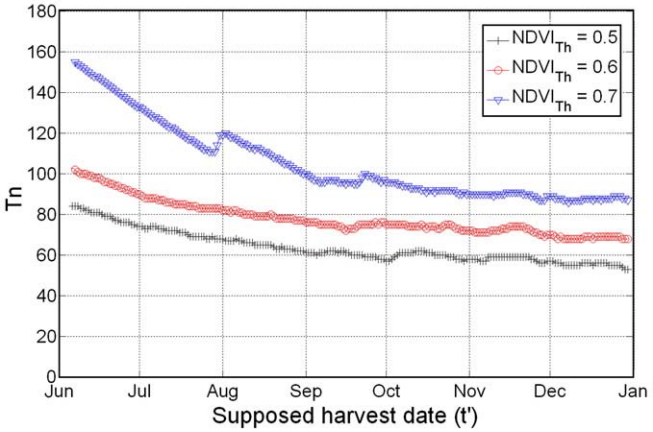

Fig. 4. Example of relationships between the supposed harvest (simulation starting date), which is the acquisition date t', and the nominal time Tn required to reach a given NDVI threshold $\mathrm{NDVI_{Th}}$.

Table 2
Characteristics of each input of the decision support system.

System input	Definition	Source(s)	Labels	Ambiguity range (for fuzzy inputs)	Explanation
In1	t vs. $[T_{LC}; T_O] \cup [T_O; T_C]$	TS EK	"No Campaign"; "Current Campaign"	–	Temporal label assigned to t according to two intervals defined by T_{LC}, T_O and T_C.
In2	t' vs. $[T_{LO}; T_{LC}] \cup [T_{LC}; T_O] \cup [T_O; T_C]$	TS EK	"No Campaign"; "Current Campaign"; "Preceding Campaign"	–	Temporal label assigned to t' according to three intervals defined by T_{LO}, T_{LC}, T_O and T_C.
In3	$(t - \text{LHD})$ vs. NCL	TS EK	"Less than Cycle Length"; "Higher that Cycle Length"	$+/-1$ month	Comparison of the difference between t and LHD to NCL (set to 9 months).
In4	$(t - t')$ vs. Tn	TS CM	"Higher than Tn"; "Less than Tn"	$+/-1$ month	Comparison of the difference between t and t' to the model indicator Tn calculated for "Supposed" harvest date $= t'$. When $(t - t')$ is "Higher than Tn" then field harvest is possible. This parameter is useful when t and t' belong to Current Campaign.
In5	$(t - T_O)$ vs. Tn	TS CM	"Higher than Tn"; "Less than Tn"	$+/-1$ month	Comparison of the difference between t and T_O with the model indicator Tn. When $(t - T_O)$ is "Higher than Tn" then field harvest is possible. This parameter is useful when $t \in$ Current Campaign and t' belong to No Campaign.
In6	$NDVI_t$	TS EK	"Low"; "Medium"; "High"	$+/-0.1$	Fuzzy set label assigned to the NDVI field value at t: "Low" if NDVI value is less than 0.3, "Medium" if it is between 0.3 and 0.75, and "High" if it exceeds 0.75.
In7	$NDVI_{t'}$	TS EK	"Low"; "Medium"; "High"	$+/-0.1$	Fuzzy set label assigned to the NDVI field value at t': "Low" if NDVI value is less than 0.3, "Medium" if it is between 0.3 and 0.75, and "High" if it exceeds 0.75.
In8	$\text{Card}(t'')\|NDVI_{t''}$ is "High"	TS EK	"No t''"; "For at least one t''"; "For the majority of t''"; "For all t''"	–	A label representing the number of t'' at which NDVI field value is "High".
In9	$(NDVI_t - NDVI_{t'})$ vs. $\Delta NDVI_{Threshold}$	TS	"Less than Threshold"; "Higher than Threshold"	$+/-0.1$	Comparison of the difference between NDVI values at t and t'' with a threshold $\Delta NDVI_{Threshold}$ set to 0.3. An important decrease in NDVI can be a good indicator for harvest detection when t and t' are too close, e.g. $(t - t') < 2$ months.
In10	$\text{Card}(t'')\|\frac{NDVI_{t'} - NDVI_{t''}}{t' - t''} > 0$	TS	"No t''"; "For at least one t''"; "For the majority of t''"; "For all t''"	–	A label representing the number of t'' at which the sign of the NDVI gradient (calculated with the consecutive date) is positive.
In11	$\text{Card}(t'')\|\frac{NDVI_{t'} - NDVI_{t''}}{t' - t''} < 0$	TS	"No t''"; "For at least one t''"; "For the majority of t''"; "For all t''"	–	A label representing the number of t'' at which the sign of the gradient (calculated with the consecutive date) is negative

t = current acquisition date, t' = previous acquisition date, t'' = all the acquisition dates preceding t' and belonging to the same temporal class, LHD = Last harvest date of the field, NCL = nominal cycle length, T_O = beginning date of the current harvest campaign, T_C = end date of the current harvest campaign, T_{LO} = beginning date of the preceding harvest campaign, T_{LC} = end date of the preceding harvest campaign, TS = Time series of satellite images, CM = Crop growth model, EK = Expert knowledge.

As can be seen in Table 2, TS contributes to the definition of all inputs by providing NDVI values or acquisition dates. EK is used in the majority of input definitions either by integrating information about cropping systems (beginning and end dates of the current harvest campaign, T_O and T_C respectively; beginning and end dates of the preceding harvest campaign, T_{LO} and T_{LC} respectively; Nominal cycle length, NCL; Last harvest date, LHD) or by its role in the configuration of fuzzy partitions. To give an example, the NDVI fuzzy sets are designed

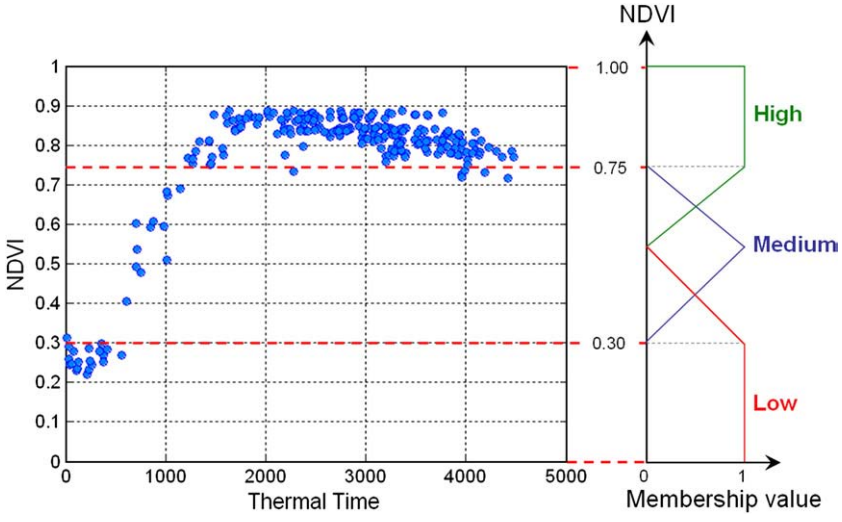

Fig. 5. NDVI profiles plotted according to thermal time for several sugarcane fields. Fuzzy sets of the NDVI defined for inputs In6 and In7 of the system are plotted on the right side.

according to expert knowledge about the phenology and field status of sugarcane as well as about its NDVI temporal profiles. The following are expert conclusions:

- *Low* NDVI values (less than 0.30) generally correspond to residues and bare soil after field harvesting.
- *Medium* NDVI values (between 0.30 and 0.75) are observed during the growth and senescence stages.
- *High* NDVI values (higher than 0.75) are observed at the end of the growth stage and before senescence.

Fig. 5 illustrates the fuzzy sets of NDVI and an example of NDVI profiles plotted according to thermal time for several sugarcane fields.

CM contributes to two inputs (In4 and In5) that evaluate harvest possibilities by comparing temporal information. An ambiguity range of ± 1 month was added to these inputs to cope with the imprecision of the model and with the effects of climatic variation observed for high values of the NDVI threshold.

Partitions of In1 and In2 are shown in Fig. 6; fuzzy sets of inputs In3, In4, In5 and In9 are shown in Fig. 7, and those of In6 and In7 are shown in Fig. 5.

5.2.2. System output

The following are three conclusions about sugarcane filed status concerning harvest events:

- *Harvested* (H) when the sugarcane field is harvested between t and t'.
- *Not harvested* (NH) when the sugarcane field is not harvested between t and t'.
- *Unknown* (U) when the status of the sugarcane field between t and t' is unknown.

Outputs of the decision support system are membership degrees (μ_H, μ_{NH} and μ_U) of the three possible conclusions (Fig. 8). These membership degrees (between 0 and 1) can be seen as confidence values assigned to the three different possibilities.

5.2.3. Rule base

Based on expert knowledge, we defined a set of 116 "If-Then" rules to link the linguistic labels of inputs to those of outputs. These linguistic rules include different scenarios that aim to cover all possible cases the system can review. Fifty-six rules corresponded to field harvest scenarios, 37 to no harvest scenarios, and 23 to scenarios with unknown conclusions. Below is an example:

- if In1 is "Current Campaign" and In2 is "No Campaign" and In3 is "Higher than Nominal Cycle Length" and In6 is "Low" and In7 is "High" then Conclusion is "Harvested"

This example illustrates the situation when t is in the current harvest campaign, t' is in the interval separating harvest campaigns, the sugarcane age is higher than the nominal cycle length, and the NDVI value at t and t' is low and high respectively; in this case it is very possible that the sugarcane field is being harvested between t and t'.

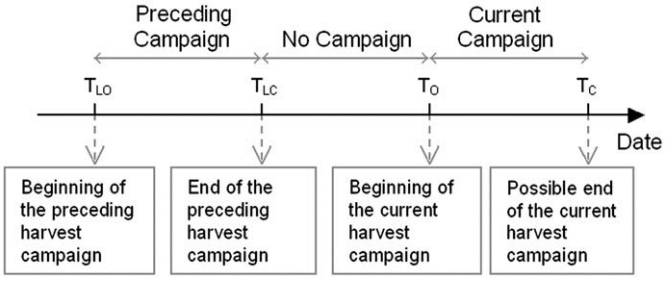

Fig. 6. Temporal intervals used for the classification of image acquisition dates. T_{LO}, T_{LC}, T_O and T_C are opening and closure dates of the preceding and the current campaign respectively.

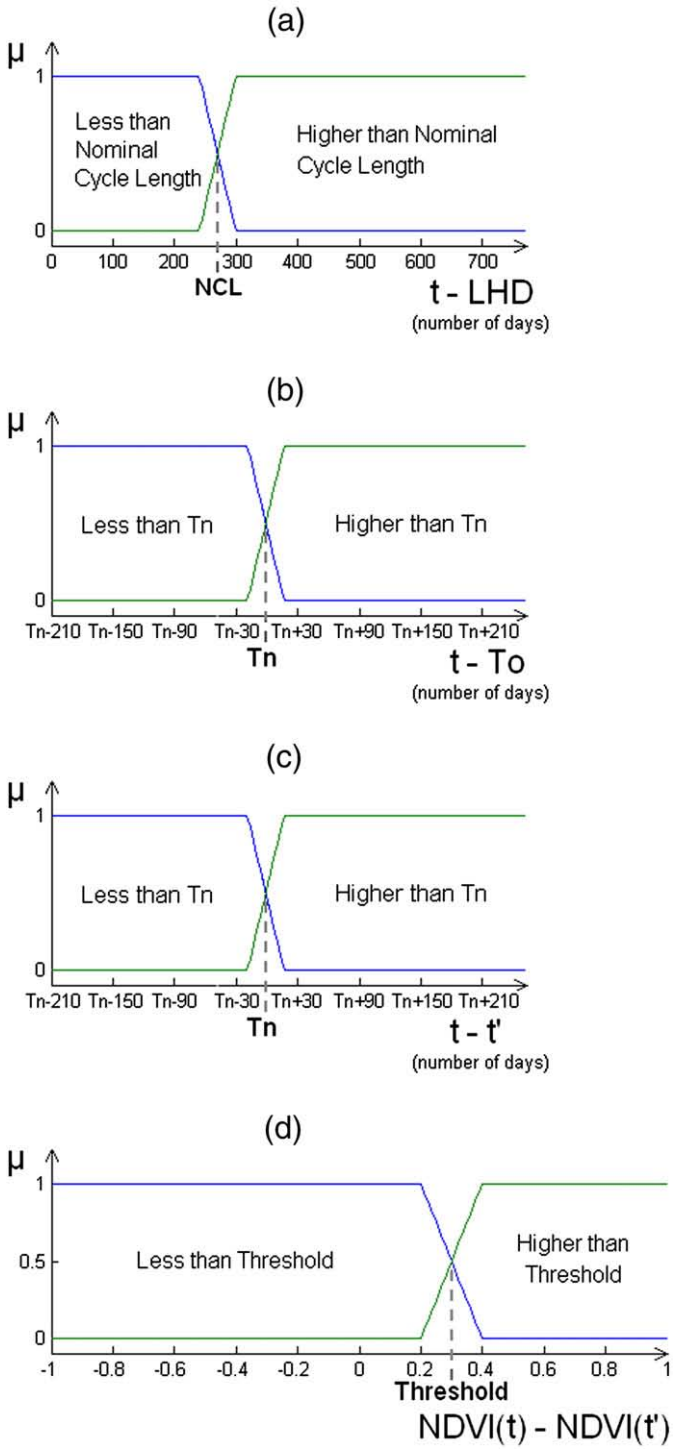

Fig. 7. Fuzzy sets of inputs In3 (a), In4 (b), In5 (c) and In9 (d). LHD = Last harvest date, NCL = Nominal cycle length, Tn = Nominal time, To = opening mill date, and Threshold = $\Delta NDVI_{Threshold}$.

5.2.4. Inference

The inference technique used in the decision support system is based on Mamdani's method (Mamdani & Assilian, 1975). The conjunction operator used to attribute the weight w^r to the conclusion $C^r \in \{H, NH, U\}$ of the fired rule r is the min, so w^r is defined as follows:

$$w^r(C^r) = \min\left(\mu_{A_1^r}(In_1), \ldots, \mu_{A_n^r}(In_n)\right) \quad (6)$$

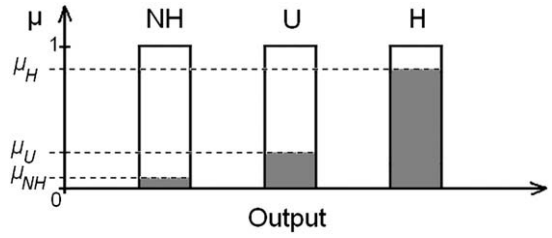

Fig. 8. Output of the support decision system. NH = "Not harvested", U = "Unknown", and H = "Harvested".

where $\mu_{A_i^r}(\mathrm{In}_i)$ is the membership degree of the input In_i's value to the fuzzy set A_i^r; for non-fuzzy inputs $\mu_{A_i^r}(\mathrm{In}_i)$ is either zero or 1 (binary membership).

The operator used to aggregate the weighted conclusions w^r of all fired rules is max. The membership degree μ_j attributed to each possible conclusion j is defined as follows:

$$\forall j = \mathrm{H}, \mathrm{NH}, \mathrm{U} \;;\; \mu_j = \left\{ \max_r \left(w^r \left(C^r \right) \right) | C^r = j \right\} \tag{7}$$

5.3. Decision making

Using the system outputs (μ_H, μ_{NH} and μ_U), users (i.e. decision makers) can make decisions according to their own approach. One decision approach could be to choose the conclusion that has the higher membership degree (Eq. (8)). Another decision approach could be based on the stability of the H and NH conclusions (e.g., Eq. (9)).

$$Decision = \arg\max(\mu_H, \mu_{NH}, \mu_U) \tag{8}$$

$$Decision = \arg\max(Stability_H, Stability_{NH}); \quad Stability_x = \mu_x - \mu_U \tag{9}$$

The decision approach that we used in this study is based on system outputs (μ_H, μ_{NH} and μ_U) as well as on a confidence level threshold μ_{conf} (Eq. (10)).

$$Decision = \begin{cases} \arg\max(\mu_H, \mu_{NH}) & \text{if } (\max(\mu_H, \mu_{NH}) \geq \max(\mu_U, \mu_{conf})) \\ U & \text{otherwise} \end{cases} \tag{10}$$

According to this approach, to decide whether a field has been harvested (H) or not (NH), first, μ_H or μ_{NH} must be higher than μ_U, meaning that there is more evidence to support a decision than to label the field status "Unknown" (U), and μ_H or μ_{NH} must be higher than a user defined confidence threshold μ_{conf}.

6. Results and discussion

The decision support system was used to automatically detect the harvest of sugarcane fields at the study site using the 18 SPOT-5 images in the time series acquired over two years: 2003 and 2004. Decisions obtained with different values of μ_{conf} were then compared to ground truth data, and error matrices were calculated.

In the following section we describe the performances of the decision support system as well as the contribution of the fuzzy sets.

6.1. System performance

The system performances were evaluated in an operational context; the images in the time series were added one by one. Each time a new satellite image were available the system decides for each cloud-free field whether it was harvested or not between the new image date and the previous cloud-free image date. Daily climatic data recorded until the new image date was used to run the crop growth model; the soil parameters were the same for the hall fields of the study site. It should be underlined that the uncertainty induced when applying the crop model to fields with different soil types and/or with different varieties is handled thanks to the use of fuzzy sets in the partitions of the indicators related to the crop growth model.

Table 3
The confusion matrix of the sugarcane harvest detection (given in number of fields times the number of dates).

		Expert system decision			Row total	Producer's accuracy (%)	Errors of omission (%)
		Harvested ($\mu_H>0$)	Not harvested ($\mu_{NH}>0$)	Unknown			
Ground truth	Harvest	136	1	1	138	98.55	1.45
	No harvest	10	1018	14	1042	97.70	2.30
Column total		146	1019	15		Overall accuracy	Percentage of unknown
User's accuracy (%)		93.15	99.90			97.80%	1.27%
Errors of commission (%)		6.85	0.10				

6.1.1. Overall accuracy and percentage of "Unknown" decisions

Overall accuracy (OA) and the percentage of "Unknown" decisions (PU) were calculated from error matrices. Table 3 shows an example of an error matrix obtained for μ_{conf} equal to zero. The columns in Table 3 correspond to the system decisions ("Harvested", "Not harvested" or "Unknown") made for all fields at all acquisition dates, and the rows correspond to the ground truth data ("Harvested" or "Not Harvested"). Looking at the sub-matrix defined by the two rows and the two first columns, the total number of correct decisions is obtained by summing the diagonal cells; the OA is then the proportion of the total number of correct decisions to the total number of decisions. The PU is the proportion of the total number of "Unknown" decisions (sum of the third column) to the total number of decisions.

Fig. 9 shows, among other results, changes in OA and PU with μ_{conf} values. OA and PU are monotonically decreasing and increasing functions of μ_{conf} respectively, with "by μ_{conf} range" stability. This stability is due to the use of fuzzy sets in input partitions. OA and PU values are steady and very satisfactory (OA>97.1% and PU<2.3%) for μ_{conf}

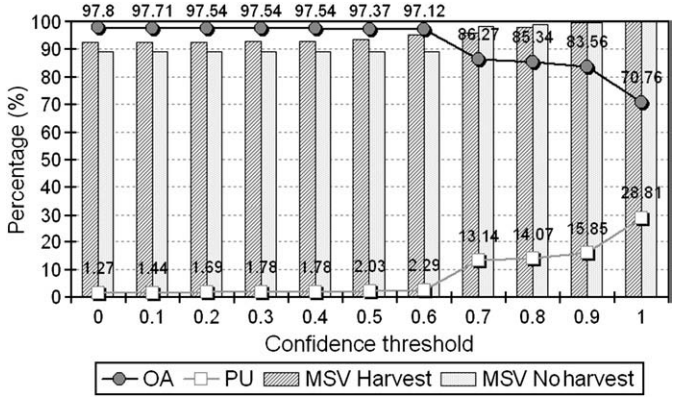

Fig. 9. System performance at different degrees of confidence threshold (μ_{conf}); OA = Overall accuracy, PU = Percentage of "Unknown", MSV Harvest = Mean stability value of decision "Harvested" and MSV No harvest = Mean stability value of decision "Not Harvested".

between zero and 0.6 (μ_H or μ_{NH} higher than 0.6). System performances drop for μ_{conf} between 0.7 and 0.9, with a decrease of about 12% in OA and an increase of about 12% in PU. This significant drop in performance is due to the fact that 10.8% of system decisions had confidence values between 0.6 and 0.7. With a μ_{conf} value equal to 1, OA and PU are 70.76% and 28.81% respectively; this is explained by the fact that 12.1% of decisions had confidence values between 0.9 and 1.

We can notice that the more the decision maker (i.e. the user) relies on the system by requiring lower confidence threshold, the better the OA and the PU. In other terms, there is no need to impose high confidence threshold, $\mu_{conf,}$, to make right decisions. This is due to the fact that the rule base used for the inference is robust and is able to manage most of all the encountered situations; i.e. even the conclusions associated to low confidence levels are correct. This robustness is also due to the fuzzy partitions. Thanks to the fuzzy formalism, small variations in the input space do not yield inappropriate changes in the output space. Moreover, the partitions, built from expert knowledge, make sense.

6.1.2. Decision stability

The stability of each H and NH decision was calculated according to the following expression:

$$\forall x = \arg\max(\mu_H, \mu_{NH}) \quad Stability(x) = \mu_x - \mu_U \tag{11}$$

Fig. 9 also shows the mean stability values (MSV) of H and NH decisions obtained for different μ_{conf} values. The MSV of both H and NH decisions decreased slightly with decreasing μ_{conf}, but even the lower values obtained (92.52% and 89.21% for MSV of H and NH respectively) reflect high stability.

6.1.3. Error analysis

Error analysis was performed to improve our understanding of the differences between decisions and ground truth data. This was done by analyzing the fired rules involved in each decision.

With μ_{conf} equal zero, the error percentage was 2.20% (26 decisions) (Table 3). Four main reasons were identified:

- Inaccuracy of harvest dates recorded by the farmer (50% of errors). This was because harvesting a field sometimes lasts several days due to rain and/or technical problems; so the farmer gave an approximate harvest date in the middle of field harvest period, which biased ground truth data.
- The lack of information about whether the sugarcane field contained a ratoon or a plantation crop (20% of errors). This information is used to set the nominal cycle length value.
- The partition configuration of some fuzzy inputs defined by expert knowledge that did not match all the specific cases and thus fired unsuitable rules (20% of errors, i.e. 5 cases). This disagreement is quite normal because the configuration of inputs, as well as the scenarios included in the rule base, only consider the most common situations.
- The harvest detection omissions that may cause future false detections (10% of errors). This error is related to the fact that the system updates the LHD (Last harvest date) value of each field according to past decisions.

For higher μ_{conf} values, the increase in the discrepancy between decisions and ground truth data was mainly due to the increase in PU values.

6.2. Contribution of fuzzy sets

The contribution of fuzzy sets to the performance of the system was assessed by comparing OA and PU values obtained using a crisp configuration with those previously obtained using a fuzzy configuration. The crisp configuration was defined by removing all ambiguity ranges from the partition of fuzzy inputs. The membership degrees assigned to the system outputs (μ_H, μ_{NH} and μ_U) with the crisp configuration are either zero or one, therefore the integration of the μ_{conf} parameter in this case was meaningless and the decision was made according to Eq. (8), argmax(μ_H, μ_{NH}, μ_U).

The OA obtained with the crisp configuration was 81.95% and the PU was 16.61%. By comparing these values to those obtained with the fuzzy configuration at the different μ_{conf} levels, we observed that the lower the level of μ_{conf} the higher the contribution of fuzzy sets; this contribution reaches 15.08% when μ_{conf} equals zero.

7. Conclusion

A novel approach for monitoring agricultural practices using time series of high spatial resolution satellite images was presented in this paper. The approach was illustrated with an application for the detection of sugarcane harvest, which is one of the most challenging change detection issues in the agricultural domain because of the high spatio-temporal variability of this crop.

A decision support system for the automatic harvest detection was described. The system deals with information from time series of SPOT-5 images by integrating crop model outputs and expert knowledge. The two latter sources of information are used to compensate for the gaps in the NDVI temporal profiles extracted from the time series and to automate the analysis of these profiles.

The formalism we used to combine heterogeneous information sources enabled the system to handle imprecise data and approximate expert reasoning. Thanks to fuzzy logic, gradualness of the data was made possible, as well as modeling linguistic terms, which helped build expert decision rules.

Unlike the wide range of bi-temporal change detection methods that have been proposed to analyze time series, the system proposed in this paper addresses the issue of temporal dependences among observations. These dependences are considered by the expert decision rules that take into account the NDVI dynamics of a sugarcane field on one hand, and the temporal constraints imposed by the crop model and by the expert knowledge, on the other hand.

The performance of the decision support system was evaluated on fields belonging to two sugarcane farms on Reunion Island. Results obtained were in substantial agreement with ground truth data: the overall accuracy reached 97.80% with stability values exceeding 92.52% and 89.21% for “Harvested” and “Not Harvested” decisions respectively. The use of fuzzy sets improved both the robustness and accuracy of the system.

The findings show that such a system is likely to fit the needs of the sugar industry for inexpensive and reliable information on the progress of the harvest throughout the milling season.

The next steps consist in analyzing the contribution of each information source to the performance of the system, and in developing an automatic method to generate interpretable decision rules using learning data.

The approach outlined in this paper is generic and very promising. Many models that simulate the growth of the main annual crops exist, e.g. INRA STICS, and expert knowledge about these crops can easily be obtained either from farmers or from agricultural knowledge bases (Russell et al., 1999). The integration of crop model outputs and expert knowledge with time series of high spatial resolution satellite images thus appears to be an excellent tool to monitor agricultural practices.

Acknowledgements

The authors thank Hélène de Boissezon (CNES) and Dr. Thierry Rabaute (CS) for their help and support, as well as Dr. Danny Lo Seen (CIRAD) and Dr. Guérric Le Maire (CIRAD) for their comments on the manuscript. The authors thank also the CNES for funding the KALIDEOS data base and for generously providing the SPOT-5 images.

References

Baldi, G., Guerschman, J. P., & Paruelo, J. M. (2006). Characterizing fragmentation in temperate South America grasslands. *Agriculture, Ecosystems & Environment*, *116*, 197−208.

Beck, P. S. A., Atzberger, C., Hogda, K. A., Johansen, B., & Skidmore, A. K. (2006). Improved monitoring of vegetation dynamics at very high latitudes: A new method using MODIS NDVI. *Remote Sensing of Environment*, *100*, 321−334.

Bégué, A., Degenne, P., Pellegrino, A., Todoroff, P., & Baillarin, F. (2004). Application of remote sensing technology to monitor sugar cane cutting and planting in Guadeloupe (French West Indies). *Geomatica* (pp. 11). La Habana, Cuba.

Bégué, A., Lebourgeois, V., Bappel, E., Todoroff, P., Pellegrino, A., Baillarin, F. et al. (Accepted for publication). Spatio-temporal variability of sugarcane fields and recommendations for yield forecast using NDVI. International Journal of Remote Sensing.

Boles, S. H., Xiao, X., Liu, J., Zhang, Q., Munkhtuya, S., Chen, S., et al. (2004). Land cover characterization of temperate East Asia using multi-temporal VEGETATION sensor data. *Remote Sensing of Environment*, *90*, 477−489.

Bouchon-Meunier, B., & Marsala, C. (2003). *Logique floue, principes, aide à la décision.* Paris: Lavoisier.

Bruzzone, L., & Smits, P. (Eds.). (2002). *Analysis of multi-temporal remote sensing images: Multitemp 2001* Singapore: World Scientific Publishing Co. Pty. Ltd.

CNES (2007). Images Spot: copyright CNES, Distribution Spot image, http://kalideos.cnes.fr

DeBoissezon, H., & Sand, A. (2006). Reference remote sensing data bases: Temporal series of calibrated and ortho-rectified satellite images for scientific use. *Proceedings of recent advances in quantitative remote sensing. Valencia, Spain*.

Delecolle, R., Maas, S. J., Guerif, M., & Baret, F. (1992). Remote sensing and crop production models: Present trends. *ISPRS Journal of Photogrammetry and Remote Sensing*, *47*, 145−161.

Dubois, D., & Prade, H. (2000). *Fundamentals of fuzzy sets.* Dordrecht: Kluwer Academic Publishers.

El Hajj, M., Bégué, A., & Guillaume, S. (2007). Multi-source information fusion: Monitoring sugarcane harvest using multi-temporal images, crop growth modelling, and expert knowledge. *MultiTemp 2007, Fourth international workshop on the analysis of multi-temporal remote sensing images. Provinciehuis Leuven, Belgium*.

El Hajj, M., Bégué, A., Lafrance, B., Hagolle, O., Dedieu, G., & Rumeau, M. (2008). Relative radiometric normalization and atmospheric correction of a SPOT 5 time series. *Sensors*, *8*, 2774−2791.

Gers, C., & Schmidt, E. (2001). Using SPOT4 satellite imagery to monitor area harvested by small scale sugarcane farmers at Umfolozi. *75th South African Sugar Technologists' Association (SASTA)* (pp. 28−33).

Gill, S. J., Milliken, J., Beardsley, D., & Warbington, R. (2000). Using a mensuration approach with FIA vegetation plot data to assess the accuracy of tree size and crown closure classes in a vegetation map of northeastern California. *Remote Sensing of Environment*, *73*, 298−306.

Gobron, N., Pinty, B., Melin, F., Taberner, M., Verstraete, M. M., Belward, A., et al. (2005). The state of vegetation in Europe following the 2003 drought. *International Journal of Remote Sensing*, *26*, 2013−2020.

Gopal, S., Woodcock, C. E., & Strahler, A. H. (1999). Fuzzy neural network classification of global land cover from a 1[degree sign] AVHRR data set. *Remote Sensing of Environment*, *67*, 230−243.

Guerif, M., Bloser, B., Atzberger, C., Clastre, P., Guinot, J. P., & Delecolle, R. (1996). Identification de parcelles agricoles à partir de la forme de leur évolution radiométrique au cours de la saison de culture. *Photo Interprétation*, *34*, 12−22.

Guerif, M., & Duke, C. L. (2000). Adjustment procedures of a crop model to the site specific characteristics of soil and crop using remote sensing data assimilation. *Agriculture, Ecosystems & Environment*, *81*, 57−69.

Guillaume, S. (2001). Designing fuzzy inference systems from data: An interpretability-oriented review. *IEEE Transactions on Fuzzy Systems*, *9*, 426−443.

Hyde, P., Dubayah, R., Walker, W., Blair, J. B., Hofton, M., & Hunsaker, C. (2006). Mapping forest structure for wildlife habitat analysis using multi-sensor (LiDAR, SAR/InSAR, ETM+, Quickbird) synergy. *Remote Sensing of Environment*, *102*, 63−73.

INRA (STICS). Simulateur mulTIdisciplinaire pour les Cultures Standard http://www.avignon.inra.fr/stics/

Laba, M., Downs, R., Smith, S., Welsh, S., Neider, C., White, S., et al. (2008). Mapping invasive wetland plants in the Hudson River National Estuarine Research Reserve using quickbird satellite imagery. *Remote Sensing of Environment*, *112*, 286−300.

Launay, M., & Guerif, M. (2005). Assimilating remote sensing data into a crop model to improve predictive performance for spatial applications. *Agriculture, Ecosystems & Environment*, *111*, 321−339.

Le Hégarat-Mascle, S., & Seltz, R. (2004). Automatic change detection by evidential fusion of change indices. *Remote Sensing of Environment*, *91*, 390−404.

Le Hegarat-Mascle, S., Seltz, R., Hubert-Moy, L., Corgne, S., & Stach, N. (2006). Performance of change detection using remotely sensed data and evidential fusion: Comparison of three cases of application. *International Journal of Remote Sensing*, *27*, 3515−3532.

Lebourgeois, V., Begue, A., Degenne, P., & Bappel, E. (2007). Improving sugarcane harvest and planting monitoring for smallholders with geospatial technology: The Reunion Island experience. *International Sugar Journal*, *109*, 109−117.

Li, Y., Vodacek, A., & Zhu, Y. (2007). An automatic statistical segmentation algorithm for extraction of fire and smoke regions. *Remote Sensing of Environment*, *108*, 171−178.

Lobell, D. B., Asner, G. P., Ortiz-Monasterio, J. I., & Benning, T. L. (2003). Remote sensing of regional crop production in the Yaqui Valley, Mexico: Estimates and uncertainties. *Agriculture, Ecosystems & Environment*, *94*, 205−220.

Lucas, R., Rowlands, A., Brown, A., Keyworth, S., & Bunting, P. (2007). Rule-based classification of multi-temporal satellite imagery for habitat and agricultural land cover mapping. *Isprs Journal of Photogrammetry and Remote Sensing*, *62*, 165−185.

Maignan, F., Breon, F. M., Bacour, C., Demarty, J., & Poirson, A. (2008). Interannual vegetation phenology estimates from global AVHRR measurements: Comparison with in situ data and applications. *Remote Sensing of Environment*, *112*, 496−505.

Mamdani, E. H., & Assilian, S. (1975). Experiment in linguistic synthesis with a fuzzy logic controller. *International Journal of Man-Machine Studies*, *7*, 1−13.

Martiné, J. F., & Todoroff, P. (2002). Le modèle de croissance Mosicas et sa plateforme de simulation Simulex: état des lieux et perspectives. *Revue Agricole et Sucrière de l'Ile Maurice*, *81*, 133−147.

Martinez-Casasnovas, J. A., Martin-Montero, A., & Casterad, M. A. (2005). Mapping multi-year cropping patterns in small irrigation districts from time-series analysis of Landsat TM images. *European Journal of Agronomy*, *23*, 159−169.

McCloy, K. R., & Lucht, W. (2004). Comparative evaluation of seasonal patterns in long time series of satellite image data and simulations of a global vegetation model. *IEEE Transactions on Geoscience and Remote Sensing*, *42*, 140−153.

Middelkoop, H., & Janssen, L. L. F. (1991). Implementation of temporal relationships in knowledge based classification of satellite images. *Photogrammetric Engineering & Remote Sensing*, *57*, 937−945.

Moulin, S., Bondeau, A., & Delécolle, R. (1998). Combining agricultural crop models and satellite observations: From field to regional scales. *International Journal of Remote Sensing*, *19*, 1021−1036.

Murthy, C. S., Raju, P. V., & Badrinath, K. V. S. (2003). Classification of wheat crop with multi-temporal images: Performance of maximum likelihood and artificial neural networks. *International Journal of Remote Sensing*, *24*, 4871−4890.

Panigrahy, S., & Sharma, S. A. (1997). Mapping of crop rotation using multidate Indian Remote Sensing Satellite digital data. *ISPRS Journal of Photogrammetry and Remote Sensing*, *52*, 85−91.

Pax-Lenney, M., & Woodcock, C. E. (1997). Monitoring agricultural lands in Egypt with multitemporal landsat TM imagery: How many images are needed? *Remote Sensing of Environment*, *59*, 522−529.

Russell, G., Muetzelfeldt, R. I., Taylor, K., & Terres, J. M. (1999). Development of a crop knowledge base for Europe. *European Journal of Agronomy*, *11*, 187−206.

Smits, P., & Bruzzone, L. (Eds.). (2004). *Analysis of multi-temporal remote sensing images: MultiTemp 2003* : World Scientific Publishing Co. Pty. Ltd.

Tapia, R., Stein, A., & Bijker, W. (2005). Optimization of sampling schemes for vegetation mapping using fuzzy classification. *Remote Sensing of Environment*, *99*, 425−433.

Turner, M. D., & Congalton, R. G. (1998). Classification of multi-temporal SPOT-XS satellite data for mapping rice fields on a West African floodplain. *International Journal of Remote Sensing*, *19*, 21−41.

Vagen, T. -G. (2006). Remote sensing of complex land use change trajectories — A case study from the highlands of Madagascar. *Agriculture, Ecosystems & Environment*, *115*, 219−228.

Woodcock, C. E., & Gopal, S. (2000). Fuzzy set theory and thematic maps: Accuracy assessment and area estimation. *International Journal of Geographical Information Science*, *14*, 153−172.

Woodcock, C. E., Macomber, S. A., Pax-Lenney, M., & Cohen, W. B. (2001). Monitoring large areas for forest change using Landsat: Generalization across space, time and Landsat sensors. *Remote Sensing of Environment*, *78*, 194−203.

Yan, H., Cao, M., Liu, J., & Tao, B. (2007). Potential and sustainability for carbon sequestration with improved soil management in agricultural soils of China. *Agriculture, Ecosystems & Environment*, *121*, 325−335.

Zadeh, L. A. (1965). Fuzzy sets. *Information and Control*, *8*, 338−353.

Zadeh, L. A. (1978). Fuzzy sets as a basis for a theory of possibility. *Fuzzy Sets and Systems*, *1*, 3−28.